International Conference on Green Energy and Environmental Engineering (GEEE-2014)
ISSN: 2356-5608
Sousse, Tunisia - 2014

Maximized Power Control based on High Order Sliding Mode for Sensorless DFIG Variable Speed Wind Turbine

Kamel Djamel Eddine KERROUCHE, Abdelkader MEZOUAR, Larbi BOUMEDIEN

Electro-technical Laboratory

Electrical Engineering Department, Faculty of Technologies
Tahar MOULAY University, Saida, Algeria

Kerrouche20@@yahoo.fr

A.mezouar@yahoo.fr

***Abstract*— The aim of this paper is to present a simple Maximized Power Control for Wind Energy Conversion System (WECS) using Double Fed Induction Generator (DFIG). The control algorithm uses High Order Sliding Mode Control technique (SMC). This control strategy, based on stator flux orientation, tracks the maximum power for different wind speeds, and regulates separately the active and reactive powers exchanged between the machine and the grid.**

Model Reference Adaptive System (MRAS) is proposed in this work for speed estimation method. The control of our system is tested under fault condition by simulation. Some results are presented and discussed to prove simplicity and efficiency of the DFIG control for WECS.

***Keywords*—DFIG, MPPT, Flux orientation, SMC, MRAS.**

I. INTRODUCTION

Wind energy is one of the most promising renewable energy sources due to the progress experienced in the last decades. Governments are attracted by the WECS with its simple structure, easy maintenance and management. With an average global annual growth rate of 14% for the period 2002-2006. Wind energy is playing a major role in the effort to increase the share of renewable energy sources in the world energy mix, helping to satisfy global energy demand, offering the best opportunity to unlock a new era of environmental protection, the world energy crises can be solved in future.

The wind turbines variable-speed operation has been used for many reasons. Among these are the decrease of the stresses on the mechanical structure, acoustic noise reduction and the possibility of active and reactive power control. Most of the major wind turbine manufacturers are developing new larger wind turbines in the 3–6-MW range. These large wind turbines are all based on variable speed operation with pitch control using a direct-driven synchronous generator (without gear box) or a doubly fed induction generator (DFIG).

Many papers have been presented, with different control schemes of WT to extract a maximum power from wind speed variable, based on fuzzy controller as it is commonly done in literature [1, 2 and 3]. The DFIG control schemes are generally based on vector control concept (with flux orientation) with Sliding Mode Control (SMC) as proposed in [4, 5]. SMC of Active and Reactive Power of a DFIG and extracting maximum power for Variable Speed by WECS in [6, 7]. Many works are done about decoupled control of DFIG to improve power quality for WECS. In [8, 9] have studied an advanced control of DFIG and power quality improvement. A suitable control for flicker problems and harmonic current are discussed in [10, 11]. DFIG during fault conditions are discussed and described in [12, 13].

An efficient MPPT technique with a suitable control approach based on sliding-mode control (SMC) is proposed in this paper for power generation control. The SMC is a kind of nonlinear control method based on a state space model of a DFIG. Control characteristics of the SMC could force the controlled variables to move along the scheduled track. The paper is organized as follows: section II presents the entire system model under study. MPPT, control strategy of DFIG and design of the SMC approach is dealt, and then is applied in section III and IV. In section V, speed estimation based on MRAS method is proposed. In section VI, some results of simulations, to validate the proposed DFIG control framework are presented and discussed.

II. WIND ENERGY CONVERSION SYSTEM

From the system viewpoint, the conversion chain can be divided into two interacting main subsystem which will be separately modeled:

- Aerodynamic Subsystem (wind turbine and gearbox),
- Electrical Subsystem (DFIG).

Fig. 1 presents a WECS, which uses DFIG.

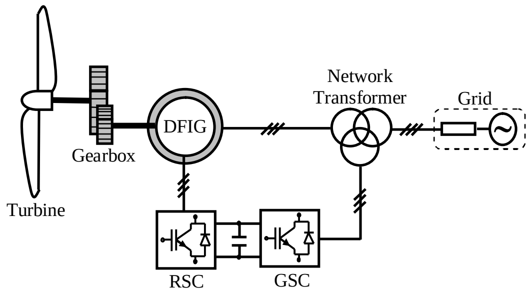

Fig. 1 Wind energy conversion chain.

A. *Aerodynamic Subsystem*

Wind turbine generation system (WTGS) convert power from the kinetic energy of the wind, thus it can be expressed as the kinetic power available in the stream of air multiplied by a C_p factor called power coefficient or Betz' s factor. The aerodynamic power is given by:

$$P_{aer} = \frac{1}{2} C_p(\lambda,\beta)\rho S V^3 \quad (1)$$

Where ρ is the air density, R is the blade length and V the wind velocity.

A wind turbine converts a certain percentage of the captured wind power. This percentage is represented by $C_p(\lambda)$ which is function of the wind speed, the turbine speed and the pith angle of specific wind turbine blades [5], [6]. This ratio is called the tip speed ratio:

$$\lambda = \frac{\Omega_t \cdot R}{V} \quad (2)$$

In a wind turbine, there is an optimum value of tip speed ratio for which C_p is maximum and that maximizes the power for a given wind speed. The turbine torque is the ratio of the aerodynamic power to the turbine shaft speed Ω_t, $T_{aer} = \frac{P_{aer}}{\Omega_t}$

Neglecting the transmission losses, the torque and shaft speed of the wind turbine, referred to the generator side of the gearbox, are given by:

$$\begin{cases} T_g = \dfrac{T_{aer}}{G} \\ \Omega_t = \dfrac{\Omega_g}{G} \end{cases} \quad (3)$$

Where T_g the driving torque of the generator and Ω_g is the generator shaft speed, respectively.

B. *Electrical Subsystem*

Using faraday's law and ohm's law, the expressions relating the voltages with the currents and fluxes across the stator winding of DFIG in the Park frame are written as follows[14]:

$$\begin{cases} v_{ds} = \dfrac{d\phi_{ds}}{dt} + \dfrac{R_s}{L_s}\phi_{ds} - \omega_s \cdot \phi_{qs} - M\dfrac{R_s}{L_s} i_{dr} \\ v_{qs} = \dfrac{d\phi_{qs}}{dt} + \omega_s \cdot \phi_{ds} + \dfrac{R_s}{L_s}\phi_{qs} - M\dfrac{R_s}{L_s} i_{qr} \\ \left(v_{dr} - \dfrac{M}{L_s} v_{ds}\right) = \sigma L_r \dfrac{di_{dr}}{dt} - M\dfrac{R_s}{L_s^2}\phi_{ds} + \dfrac{M}{L_s}\omega\phi_{qs} + \\ \qquad (R_r + \dfrac{M^2}{L_s^2} R_s) i_{dr} - \sigma L_r \omega_r i_{qr} \\ \left(v_{qr} - \dfrac{M}{L_s} v_{qs}\right) = \sigma L_r \dfrac{di_{qr}}{dt} - \dfrac{M}{L_s}\omega\phi_{ds} - M\dfrac{R_s}{L_s^2}\phi_{qs} + \\ \qquad \sigma L_r \omega_r i_{dr} + (R_r + \dfrac{M^2}{L_s^2} R_s) i_{qr} \end{cases} \quad (4)$$

Where R_s and R_r are stator and rotor resistances. L_s, L_r are stator and rotor inductances. M, σ are mutual inductance and leakage coefficient. $\omega = p \cdot \Omega_g$ is the electrical speed and p is the pair pole number, ω_r is the rotor pulsation.

The stator and rotor flux can be expressed as:

$$\begin{cases} \phi_{ds} = L_s i_{ds} + M i_{dr} \\ \phi_{sq} = L_s i_{qs} + M i_{qr} \\ \phi_{rd} = L_r i_{dr} + M i_{ds} \\ \phi_{rd} = L_r i_{qr} + M i_{qs} \end{cases} \quad (5)$$

Where i_{ds}, i_{qs}, i_{dr}, and i_{qr} are, respectively, the direct and quadrate stator and rotor currents.

The active and reactive powers at the stator and rotor, as well as those provide for grid, are defined as:

$$\begin{cases} P_s = v_{ds} \cdot i_{ds} + v_{qs} \cdot i_{qs} \\ Q_s = v_{qs} \cdot i_{ds} - v_{ds} \cdot i_{qs} \\ P_r = v_{dr} \cdot i_{dr} + v_{qr} \cdot i_{qr} \\ Q_r = v_{qr} \cdot i_{dr} - v_{dr} \cdot i_{qr} \end{cases} \quad (6)$$

The electromagnetic torque is expressed as:

$$T_{em} = p(i_{qs}\phi_{ds} - i_{ds}\phi_{qs}) \quad (7)$$

To maximize the generated power, it is therefore desirable for the generator to have a power characteristic that will follow the maximum $C_{p\max}$ line.

III. Maximum Power Point Tracking

A lot of methods on the maximum power point tracking (MPPT) have been proposed in literatures [6, 7 and 9]. The first method is simple and based on the tip speed of the wind turbine. Therefore, an anemometer is required for measuring the wind speed on the wind turbine, the optimal speed of the turbine can be determined as follows from Equation (2):

$$\Omega_{t,opt} = \frac{\lambda_{opt} \cdot V}{R} \tag{8}$$

This method needs an additional anemometer for measuring the wind speed. Thereby, it is difficult to measure the tip speed of the wind turbine. Consequently, we can conceive another method for MPPT without enslavement of speed.

This simple method consists to estimate the wind speed as follows:

$$\hat{V} = \frac{R \cdot \hat{\Omega}_t}{\lambda_{opt}} \tag{9}$$

The control objective is to optimize the capture wind energy by tracking the optimal torque $T_{aer,opt}$.

$$T_{aer,opt} = \frac{1}{2\Omega_t} C_p \rho S V^3 \tag{10}$$

For each wind speed, there is a certain rotational speed at which the power curve of a given WT has a maximum (C_p reaches its maximum value).

The block diagram of the MPPT control system for the wind turbine is shown in Fig. 2.

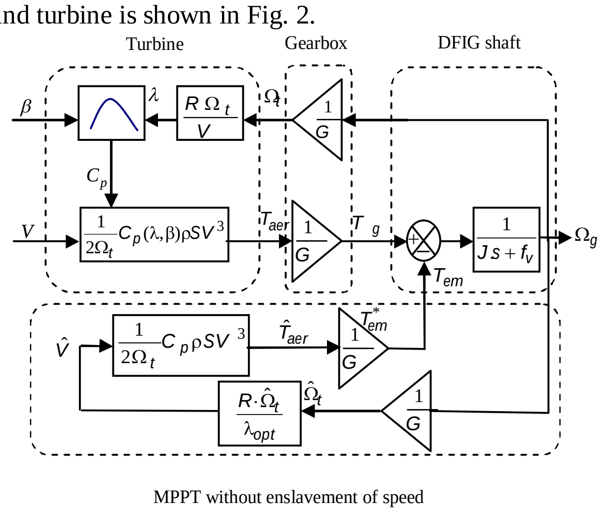

Fig. 2 The block diagram of the MPPT without enslaved speed.

The above control block diagram of variable-speed fixed-pitch WECS aims at regulating the power harvested from wind by modifying the generator speed; in particular, the control objective consist to capture the maximum power available from wind.

IV. CONTROL STRATEGY OF THE DFIG

A. *Field oriented control*

Once the DFIG is connected to an existing grid, the transit of active and reactive powers must be controlled separately. To obtain a decoupled powers control of DFIG, the method based on field orientation can be regarded as the efficient one. The principle of this method consists to orientate the stator flux in such a way that the stator flux vector points into d-axis direction, as shown in Fig. 3. This approach is realized by setting the quadratic component of the stator flux to the null value:

$$\phi_s = \phi_{ds} \quad \Rightarrow \quad \phi_{qs} = 0 \tag{11}$$

Using the condition above, supposing that the grid system is steady, having a single voltage V_s that leads to stator's constant flux ϕ_s, we can easily deduce the voltages as:

$$\begin{cases} v_{ds} = 0 \\ v_{qs} = \omega_s \cdot \phi_s = V_s \end{cases} \tag{12}$$

If per phase stator resistance is neglected, which is a realistic approximation for medium power machines used in WECS, the stator voltage vector is consequently in quadrate advance in comparison with the stator flux vector.

By using equations (12) and (4), we obtain for the rotor voltages:

$$\begin{cases} v_{dr} = \sigma L_r \dfrac{di_{dr}}{dt} + R_r i_{dr} - \sigma L_r \omega_r i_{qr} + \dfrac{M}{L_s}\dfrac{d\phi_{ds}}{dt} \\ v_{qr} = \sigma L_r \dfrac{di_{qr}}{dt} + R_r i_{qr} + \sigma L_r \omega_r i_{dr} + g\dfrac{M}{L_s} V_s \end{cases} \tag{13}$$

Where V_s is the stator voltage magnitude assumed to be constant and g is the slip range, we can rewrite the rotor voltages as follows:

$$\begin{cases} v_{dr} = \sigma L_r \dfrac{di_{dr}}{dt} + R_r i_{dr} + fem_d \\ v_{qr} = \sigma L_r \dfrac{di_{qr}}{dt} + R_r i_{qr} + fem_q \end{cases} \tag{14}$$

With fem_d and fem_q are the crosses coupling terms between the d – axis and q – axis:

$$\begin{cases} fem_d = -\sigma L_r \omega_r i_{qr} \\ fem_q = \sigma L_r \omega_r i_{dr} + s\dfrac{M}{L_s} V_s \end{cases} \tag{15}$$

Consequently, with regard to (11), the fluxes are simplified as indicated below:

$$\begin{cases} \phi_{ds} = L_s i_{ds} + M i_{dr} \\ 0 = L_s i_{qs} + M i_{qr} \end{cases} \tag{16}$$

From (16), we can deduce the currents as:

$$\begin{cases} i_{ds} = \dfrac{\phi_{ds} - M i_{dr}}{L_s} \\ i_{qs} = -\dfrac{M}{L_s} i_{qr} \end{cases} \tag{17}$$

Using Equations (6), (12) and (17) the stator active and reactive power can then be expressed only versus these rotor currents as:

$$\begin{cases} P_s = -V_s \cdot \dfrac{M}{L_s} i_{qr} \\ Q_s = -V_s \cdot \dfrac{M}{L_s}\left(i_{dr} - \dfrac{\phi_{ds}}{M}\right) \end{cases} \tag{18}$$

Using (14), (17), we obtain:

$$\begin{cases} P_s = -V_s \cdot \dfrac{M}{L_s} \dfrac{1}{(\sigma L_r \cdot p + R_r)}\left(v_{qr} - fem_q\right) \\ Q_s = -V_s \cdot \dfrac{M}{L_s} \dfrac{1}{(\sigma L_r \cdot p + R_r)}\left(v_{dr} - fem_d\right) + V_s \cdot \dfrac{\phi_{ds}}{L_s} \end{cases} \tag{19}$$

Field oriented control of the DFIG can then be applied with the active and reactive power considered as variables to be controlled. And, we consequently the bloc diagram is presented in Fig. 4.

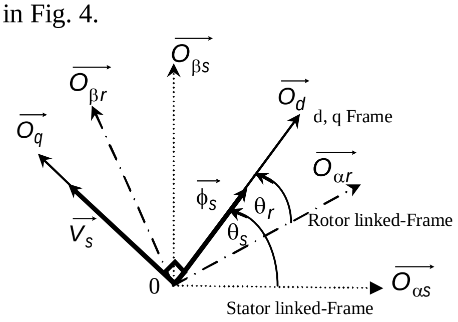

Fig. 3 Stator flux orientation.

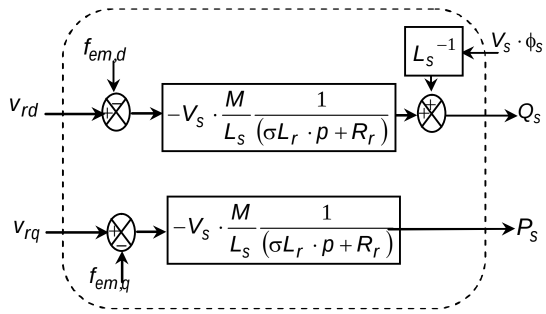

Fig. 4 The coupled model of active and reactive stator powers.

B. Sliding Mode Control (SMC)

A sliding mode controller (SMC) is a Variable Structure Controller (VSC). Basically, a VSC includes several different continuous functions that can map plant state to a control surface, whereas switching among different functions is determined by plant state represented by a switching function.

The control law satisfies the precedent conditions is presented in the following form:

$$\begin{cases} u_{dq} = u_{eq} + u_n \\ u_n = K \cdot sign(S(x,t)) \end{cases} \tag{20}$$

Where u_{dq} is the control vector, u_{eq} is the equivalent control vector, u_n is the switching part of the control (the correction factor), K is the controller gain. u_{eq} can be obtained by considering the condition for the sliding regime, $S(x,t)$ .The equivalent control keeps the state variable on sliding surface, once they reach it. For the defined function:

$$sign(\varphi) = \begin{cases} 1 \quad if \quad \varphi > 0 \\ 0 \quad if \quad \varphi = 0 \\ -1 \quad if \quad \varphi < 0 \end{cases} \tag{21}$$

The controller described by the equation (21) presents high robustness, insensitive to parameter fluctuations and disturbances, but it will have high-frequency switching (chattering phenomena) near the sliding surface due to sign function involved by introducing a boundary layer with width.

Using (20) and (21), the control law becomes [15]:

$$u_{dq} = u_{eq} + K \cdot sign(S(x,t)) \tag{22}$$

Consider a Lyapunov function:

$$V = \frac{1}{2} S(x)^2 \tag{23}$$

If the Lyapunov theory of stability is used to ensure that SMC is attractive and invariant, the following condition has to be satisfied:

$$\dot{V} = \frac{1}{2}\frac{d}{dt} S(x)^2 \le 0 \tag{24}$$

In this paper, we use the sliding surface proposed by J. J. Slotine [16]:

$$S(x) = \left(\frac{\partial}{\partial t} + \lambda_x\right)^{n-1} e(x) \tag{25}$$

Where $e(x)$ is the error vector (e (x) = x* -x), λ_x is a positive coefficient, n is the system order.

C. Application of SMC to DFIG

For $n = 2$ and using the equation (25) with satisfying the condition (24), replacing the rotor currents by their expressions given in (13), we can obtain the sliding surfaces representing the error between the measured and references rotor currents as follow:

$$\begin{cases} \dot{S}_d(Q_s) = \dot{Q}_s^* - \dfrac{3}{2}\dfrac{V_s}{L_s}\left[\lambda_Q \phi_s - \left(\dfrac{R_r}{L_r} i_{dr} - \lambda_Q\right) M i_{qr} - \omega_r M i_{qr}\right] + \lambda_Q Q_s^* + \\ \qquad \dfrac{3}{2}\dfrac{M}{L_s L_r} V_s v_{dr} \\ \dot{S}_q(P_s) = \dot{P}_s^* - \dfrac{3}{2}\dfrac{M V_s}{L_s}\left[\left(\lambda_P - \dfrac{R_r}{L_r}\right) i_{qr} - \omega_r i_{dr} - \omega_r \dfrac{M}{L_s L_r}\phi_s\right] + \lambda_P P_s^* + \\ \qquad \dfrac{3}{2}\dfrac{M}{L_s L_r} V_s v_{qr} \end{cases}$$

(30)

v_{dr} and v_{qr} will be the two components of the control vector used to constraint the system to converge to $S_{dq} = 0$.

The control vector u_{eq} is obtained by imposing $\dot{S}_{dq} = 0$. So, the equivalent control components are given by the following relation:

$$\begin{cases} v_{dr,eq} = \dfrac{2}{3}\dfrac{L_s L_r}{M V_s}\left[\dot{Q}_s^* + C_Q\left(Q_s^* - Q_s\right)\right] + R_r i_{dr} - L_r \omega_r i_{qr} \\ v_{qr,eq} = \dfrac{2}{3}\dfrac{L_s L_r}{M V_s}\left[\dot{P}_s^* + C_p\left(P_s^* - P_s\right)\right] + R_r i_{qr} + \dfrac{M}{L_s}\omega_r \phi_s + L_r \omega_r i_{dr} \end{cases}$$

(31)

V. SENSORLESS BASED MRAS

From equation (6), Assuming that the losses in the inverter are neglected, so, the out voltages are the references, the reference power model is:

$$Q_r^* = v_{qr}^* \cdot i_{dr} - v_{dr}^* i_{qr} \qquad (32)$$

Substituting (4) with the application of the flux orientation, the expression at the steady state of the reactive power is:

$$\hat{Q}_r = \hat{\omega}_r \left[\sigma L_r I_r^2 - \frac{M}{L_s}\phi_s i_{dr} \right] \qquad (33)$$

The error (ε) between the two models is passed through the adaptation mechanism (a PI controller). The output of the PI controller is the estimated slip speed $\hat{\omega}_r$, which is then used to tune the adjustable model such that error (ε) converges to zero.

Equation (22) shows the Adaptive System model which is independent of the rotor resistance. This leads to higher accuracy of the speed estimation regardless any variations in rotor resistance. The proposed MRAS observer scheme is shown in Fig. 5.

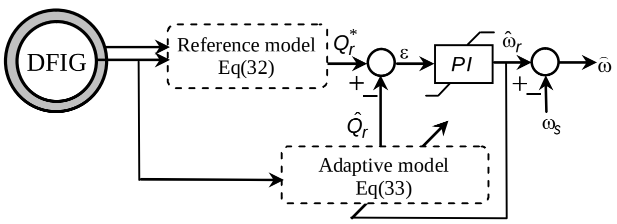

Fig. 5 Reactive stator power based MRAS observer.

VI. SIMULATIONS RESULTS:

In this section, we will study a low-power variable-speed fixed-pitch WECS. The parameters of the WECS are shown in Appendix.

The wind profile used in our simulations is shown in Fig. 6 (a). The whole system is tested under fault condition of the stator voltage with a drop around 25% of 0.5 s between 1.5s and 2.0 s, except this disturbance, the machine is considered as working over ideal conditions (no perturbations and no parameters variations).

To guarantee a unity power factor at the stator side, the reactive power is maintained to zero. The stator active and reactive powers are controlled according to the MPPT and sliding mode control strategy.

Fig. 6 (b) shows that the estimated generator shaft speed coincides with the actual speed, which is proportional to the curve of the wind speed.

Fig. 6 (c) and 6 (d) show the rotor currents.

For the active and reactive stator powers, shown in Fig. 6 (e), 6 (f), we notice a very good tracking of the stator active power injected into the grid, except the presence of a very small oscillations in the occurrence of the fault. The stator reactive power maintained at zero, which guarantees a unitary power factor at the stator side.

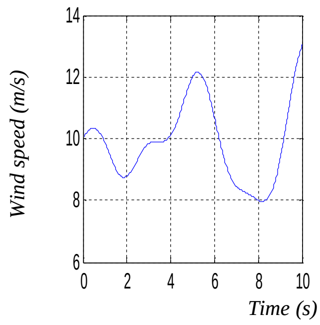

(a) Generator shaft speed.

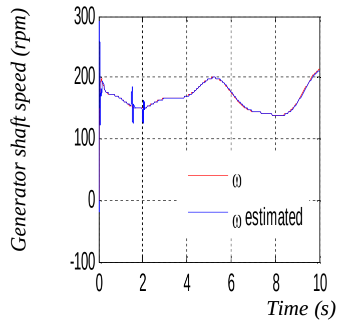

(b) Electromagnetic torque.

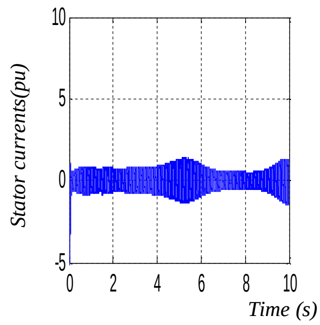

(c) Rotor Currents.

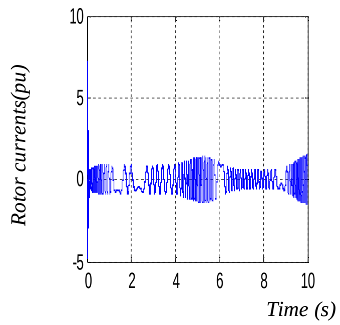

(d) Stator Currents.

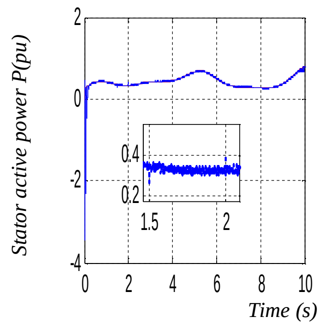

(e) Reference and stator active powers.

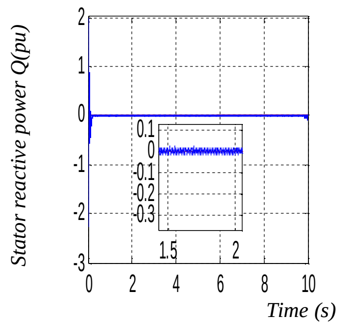

(f) Reference and stator reactive powers.

Fig. 6 Responses of the WECS.

VII. CONCLUSION

In this paper, we have presented a robust control of wind energy conversion system with DFIG connected to the grid, using MPPT technique and flux orientation. The MPPT technique has been successfully applied for generate reference for active power to be tracked. The control based on stator flux orientation, is simply realized by high order sliding mode controller. Simulations results have shown good performances for the controller in the presence of wind speed variation and voltage drop. It has been also developed a new speed estimation using MRAS-Based approach. It is, however, been claimed that the proposed MRAS observer robust against voltage drop.

APPENDIX

In this part, simulations are investigated with a 1.5MW generator connected to a 690V/50Hz grid. The machine's parameters are presented below:

Three pole pairs, Rs = 0.012Ω, R_r = 0.021 Ω, M= 0.0135 H, L_s= M+2.00372 e-4 H, L_r= M+1.7507 e-4 H,

Turbine’s parameters: diameter=35 m, number of blades = 3, gearbox ratio = 90.

J : Inertia (turbine+DFIG) = 100 Kg.m2 and f : viscous coefficient (turbine+DFIG) = 0.0024Kg.m/s.

REFERENCES

[1] V.Calderaro, V.Galdi, A.Piccolo, P.Siano, “A fuzzy controller for maximum energy extraction from variable Speed wind power generation systems”, Electric Power Systems Research, Vol.78, 2008, pp 1109–1118.

[2] V. Galdi , A. Piccolo , P. Siano, “Exploiting maximum energy from variable speed wind power generation systems by using an adaptive Takagi–Sugeno–Kang fuzzy model”, Energy Conversion and Management, Vol 50, Issue 2, 2009, pp 413–421.

[3] Ali M. Eltamaly,Hassan M. Farh, “Maximum power extraction from wind energy system based on fuzzy logic control”, Electric Power Systems Research, Vol. 97, 2013, pp 144– 150.

[4] M. Machmoum, F. Poitiers, Sliding mode control of a variable speed wind energy conversion system with DFIG, International Conference and Exhibition on Ecologic Vehicles and Renewable Energies, MONACO, March 26-29 (2009).

[5] M. Abid, A. Mansouri, A. Aissaoui, B. Belabbes, Sliding mode application in position control of an induction machine, J. Electr. Engin., Vol. 59, N°. 6, pp. 322-327, 2008.

[6] B. Beltran, T. Ahmed-Ali, and M.E.H. Benbouzid, “Sliding mode power Control of variable speed wind energy conversion systems,” IEEE Trans. Energy Convers., vol.23, no.22, pp.551–558, Jun.2008.

[7] Y. Bekakra, D. Ben Attous, Sliding Mode Controls of Active and Reactive Power of a DFIG with MPPT for Variable Speed Wind Energy Conversion, Australian Journal of Basic and Applied Sciences, Vol. 5, N°. 12, pp. 2274-2286, 2011.

[8] F. Poitiers, T. Bouaouiche, M. Machmoum. Advanced control of a doubly-fed induction generator for wind energy conversion. Electric Power Systems Research 79 (2009) 1085–1096.

[9] M.Boutoubat, L.Mokrani, M.Machmoum. Control of a wind energy conversion system equipped by a DFIG for active power generation and power quality improvement. Renewable Energy 50 (2013) 378e386.

[10] A. Gaillard, P. Poure, S. Saadate, M. Machmoum. “Variable Speed DFIG Wind Energy System for Power Generation and Harmonic Current Mitigation”. Renewable Energy 34,2009 pp 1545-1553.

[11] T.K.A. Brekken, N. Mohan. Control of a doubly fed induction wind generator under unbalanced grid voltage conditions. IEEE Transaction on Energy Conversion 22 (March (1)) (2007) 129–135.

[12] Z.Song, Ch.Xia , T.Shi. Assessing transient response of DFIG based wind turbines during voltage dips regarding main flux saturation and rotor deep-bar effect. Applied Energy 87 (2010) 3283–3293.

[13] L. Piegari, R. Rizzo. A control technique for doubly fed induction generators to solve flicker problems in wind power generation. International Power and Energy Conference. Putrajaya: Malaysia; 28 and 29 November 2006 pp. 19–23.

[14] B.Robyns, B.Francois, Ph.Degobert, J.P.Hautier, Vector control of induction machines, Springer-Verlag London 2012..

[15] A. Mezouar, M.K. Fellah, S. Hadjeri, « Adaptive sliding mode observer for induction motor using two-time-scale approach », Electric Power Systems Research (Elsevier), (DOI:10.1016/j.epsr.2006.05.010), 2006.

[16] J. J. Slotine, W. Li, “Applied non-linear Control”, Prentice-Hall Edition, 1991.